EXHIBIT 4

Harvard Medical School
Harvard TH Chan School of Public Health

John J. Godleski, M.D.
Professor of Pathology Emeritus

Department of Environmental Health (MIPS Program)

jgodlesk@hsph.harvard.edu
Phone (617) 698-5970
Cell (617) 840-9679

July 12, 2021

David Dearing. ESQ
Beasley Allen Law Firm
218 Commerce Street
Montgomery, AL 36104

Re: Hiliary Converse

Dear Mr. Dearing:

I was on the faculty of Harvard Medical School (HMS), Brigham and Women's Hospital (BWH), and Harvard School of Public Health (HSPH) from 1978-2017, retiring as Professor of Pathology in 2017. I graduated from the University of Pittsburgh School of Medicine. As a student, I did research in the Pathology Department learning electron microscopy. In my senior year, I received the top award for research done by a medical student in the United States given by the Student American Medical Association, and published several papers describing that research. I then did an internship and residency in Pathology at the Massachusetts General Hospital, a major teaching hospital of Harvard Medical School. I received further training at HSPH and the University of North Carolina. I was board certified in Anatomic Pathology in 1975. I spent 5 years on the faculty of Medical College of Pennsylvania in Philadelphia in the Department of Pathology where I was in charge of the electron microscopy facility and the autopsy service, and then was recruited to head Pulmonary Pathology at BWH in Boston, a position I held for 37 years. I published more than one hundred and seventy peer-reviewed papers related to pulmonary/environmental pathology including a number using analytical electron microscopy. Notably, I have been senior author on a number of papers using analytical electron microscopy with both X-ray analysis and electron energy loss spectroscopy. In my career, I received more than $30 million in research grants from NIH, EPA, and other funding agencies as Principal Investigator; I led the Particles Research Core in the Harvard-NIEHS Environmental Research Center and I was Associate Director of the Harvard Clean Air Research Center supported by the US EPA. In my daily activities, I was a member of the Pulmonary Pathology and Autopsy Services at Brigham and Women's Hospital. I taught Pathology residents and fellows, medical students, graduate students, and postdoctoral fellows, and I carried out research in my laboratory at HSPH. I was responsible for accurate pathological diagnoses at BWH and I oversaw a research group of as many as 15 people at HSPH. I was the pathologist providing the final opinion on difficult diagnostic cases of lung disease within our department, and I was a recognized expert whose opinion was sought by pathologists from other hospitals in the diagnosis of foreign material in tissues throughout the body using scanning electron microscopy (SEM) and energy dispersive X-ray analyses (EDS). Although now retired, I have full access to laboratory and electron microscopy facilities.

I have recently published six papers regarding talc and tissue pathology (references 1-6). The first paper used tissue digestive procedures and SEM/EDS to quantify talc in lymph nodes in comparison to the use of *in situ* SEM/EDS; the second described the migration and detection of talc in pelvic tissues from the perineum in a series of exposed patients who also had ovarian malignancy. The third concerned the use of spectroscopic magnesium and silicon weight % ratio standards to diagnose talc in human tissues, and

the expected mathematical distribution for such measurements. Three other publications also pertain to talc identification in tissue and resultant pathology (references 4-6).

I have reviewed 42 out of a possible 42 hematoxylin and eosin (H&E)-stained slides, plus three additional H&E recuts on block 1-FS1 (therefore, total of 45 slides) on Hilary Converse (S07-31005). These represent the tissues from the patient's surgical procedure on 9/5/2007 which consisted of a hysterectomy, bilateral salpingo-oophrectomy, excision of bilateral pelvic and para-aortic lymph nodes, and peritoneal and diaphragm biopsies. Slides on this case were received with the following sublabels: 1-(1 through 6, plus the frozen section remnant slides), 2-(1 through 8), 3-(1 through 8), 4-(1 through 5), 5-(1 through 5), 6-(1 through 2), 7-1, 8- (1 through 3), 9-(1 through 2), and 10-(1 through 2). In addition, the slides' sublabels included a short one-to-three letter/number designation intended to reflect the anatomic site, e.g. OV for ovary, LN for lymph node and C12 for anterior cervix. All slides were prepared by the Department of Pathology at Yale Medical Center, 20 York St. EP 2-607, New Haven, CT 06510. The histologic slides listed above were reviewed with light microscopy, and the diagnosis of clear cell carcinoma of the ovary was confirmed. In the surgical pathology report, the tumor was described as being in the left ovary and having a maximum dimension of 12.5 cm, without involvement of the ovarian surface, the contralateral ovary, or either fallopian tube. The pathologic tumor stage was given in the report as pT1a N0 MX. Also received were 11 slides from case N07-5280, which represent cytology specimens (pelvic wash, right pericolic wash, and left pericolic wash) taken from Ms. Converse on the same day as the main hysterectomy specimen (9/5/2007). These slides were reviewed and confirmed the diagnosis of negative for malignant cells. Also received were 41 paraffin tissue blocks on S07-31005 and three paraffin blocks on N07-5280, corresponding to the cases described above. **Figure 1** illustrates key microscopic findings. In the photographs within that figure are shown typical areas of the patient's clear cell carcinoma.

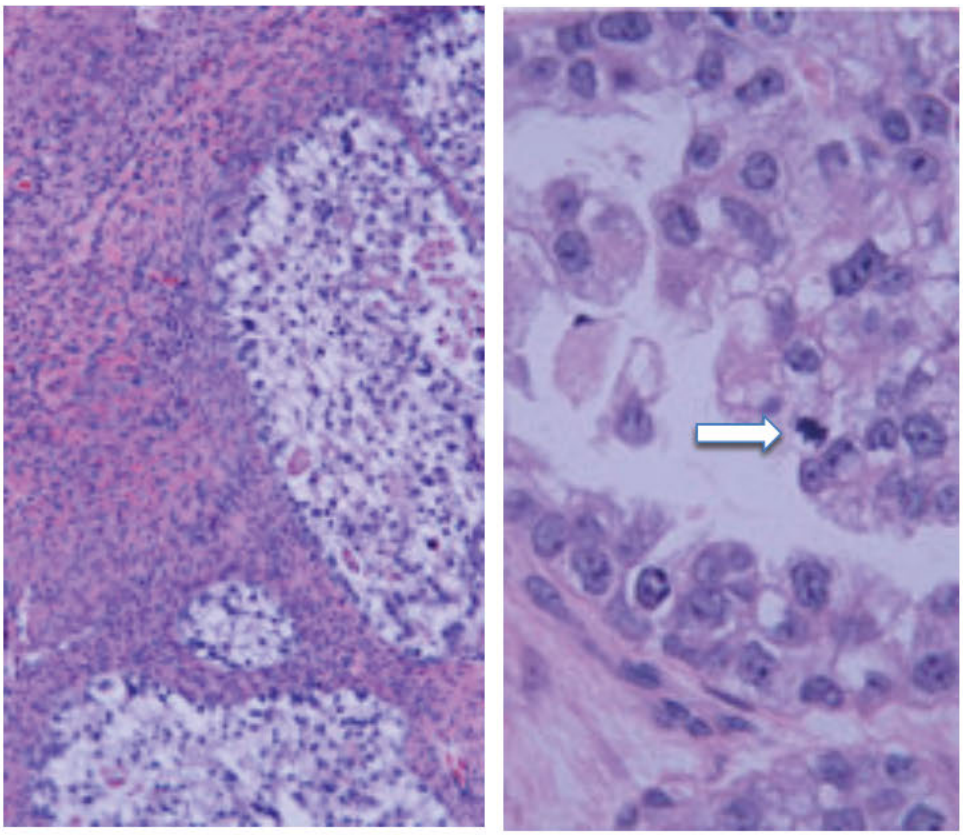

Figure 1. Left. Low-power microscopic view of the patient's clear cell carcinoma of the ovary, showing a nesting architecture, and with benign ovarian fibrous stroma present (left side of image). The tumor shows a poorly differentiated architecture. Original magnification 60x. **Right**. High-power view of the clear cell carcinoma in this case, showing moderate nuclear pleomorphism and the cytoplasmic clear cell morphology, which is a hallmark of this tumor type. A mitotic figure is shown (arrow). Original magnification 400x. Hematoxylin-eosin stain.

The 45 H&E histologic slides on case S07-31005 were also reviewed using polarized light microscopy, as a means to highlight and detect birefringent foreign material in the same plane of focus with the tissues. Birefringent particle(s) were observed in 25 of the 45 slides reviewed. In **Figure 2,** two photos are shown

with birefringent particles (highlighted by polarized light microscopy) in the same plane of focus with the tissues.

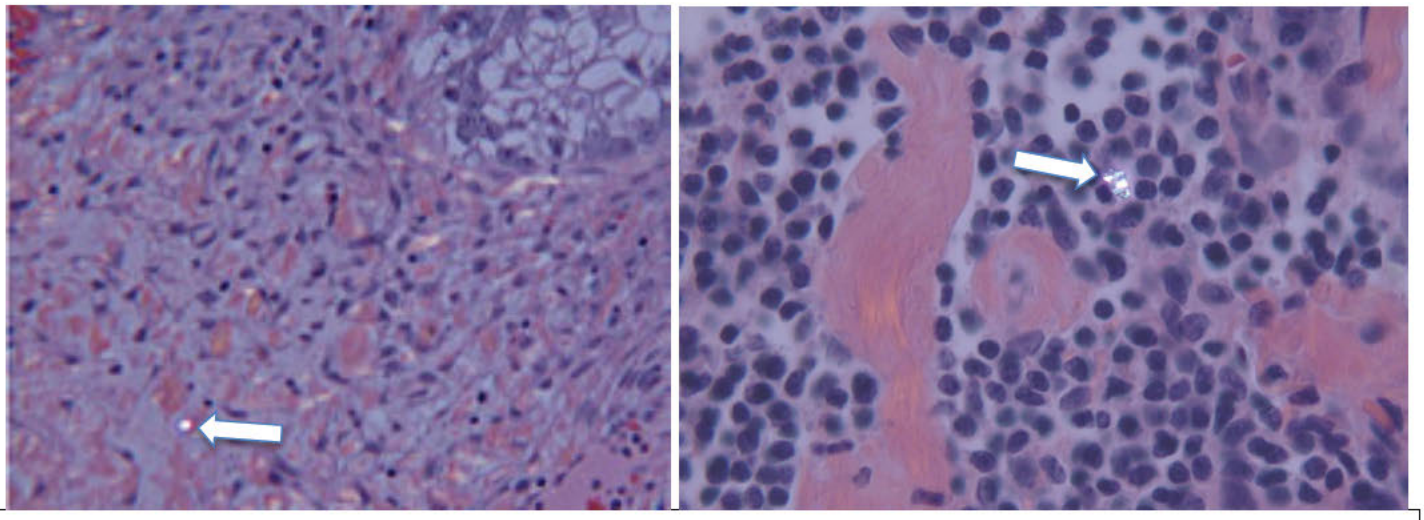

Figure 2. Left. Tissue from the left ovary, with a birefringent particle present within densely fibrotic stroma (see arrow) in the plane of focus with the tissues. An ovarian tumor nest is at top right. Original magnification 160x. **Right**. Tissue from a right pelvic lymph node showing birefringent particles/fibers (see arrow) in the plane of focus with the tissues. Original magnification 400x. All sections stained with hematoxylin-eosin; and with polarized light microscopy.

Our past experience and the medical literature on the diagnosis of talc in tissues (see references) indicate that the number of birefringent particles in histological sections is robustly correlated with the number of talc particles found by SEM/EDS, since talc is a strongly birefringent material. Also, talc is more likely to be subsequently found by SEM/EDS in tissue sections where 1) the number of birefringent particles by polarized light microscopy is greatest, and 2) the anatomic location of the tissues is most consistent with the expected migration or dissemination patterns for the talc, given its initial application/exposure site (references 1-2).

Taking these factors into consideration, seven paraffin tissue blocks from Ms. Converse's 9/5/2007 surgery (3-4LN, 2-7OV, 2-8OV, 2-2C12, 1-4OV, 8-2LN, and 8-3LN), representing left ovary (1-4OV), right ovary and fallopian tube (2-7OV, 2-8OV), anterior cervix (2-2C12), right pelvic lymph node (3-4LN) and right para-aortic lymph nodes (8-2LN, 8-3LN), were selected for further studies. All seven of these paraffin tissue blocks were studied by the *in situ* scanning electron microscopy technique using variable pressure as described by Abraham and Thakral (2007, reference 6), in which the paraffin block may be studied directly in the scanning microscope chamber. The blocks were handled with our standard protocol to prevent contamination of the blocks in our laboratory. This protocol begins with the handling of the blocks using powder-free gloves on pre-cleaned surfaces. The blocks were then sectioned, removing ~50 micrometers of tissue and paraffin using a rotary microtome with a new, stainless steel blade. This sectioning was done to remove any surface contamination from previous storage and handling. After the fresh surface was exposed, the blocks were washed in distilled water for $\geq$2 minutes to remove soluble surface materials such as sodium chloride and sodium phosphate used in processing for histology. Then the blocks were placed in a clean covered container to prevent air particulate contamination, and then transferred to the electron microscopy facility. There, blocks were again handled with particle-free gloves on pre-cleaned surfaces. When not being examined in the SEM chamber, the blocks were always maintained in closed plastic stub container boxes to provide secure storage and to obviate lab contamination. An example of a paraffin block studied in this case is shown in **Figure 3**.

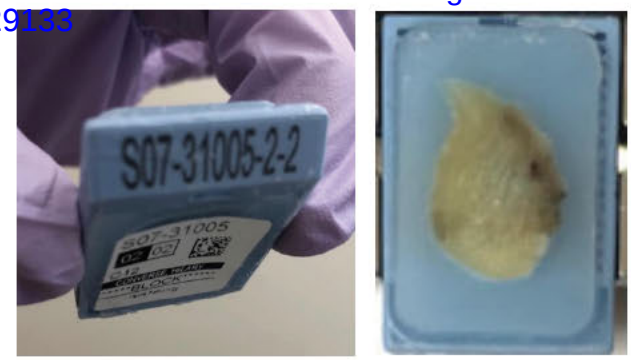

Figure 3. One of the blocks (2-2C12, anterior cervix) examined by SEM/EDS in this case. **Left:** The labeling (identification) for the block, which is on the side and bottom of the cassette. **Right:** Picture of the cut tissue surface of the block (examined by SEM/EDS).

Tissue surfaces were studied with a JEOL JSM IT500HR field emission SEM with attached Oxford energy dispersive X-ray analysis system (EDS), with Oxford instrument software being Aztec 3.3 and EDS detector model being X-Max 150. The backscatter mode of the microscope was used to highlight mineral particles within the tissue resulting from atomic number contrast. Areas of tissue in the sectioned block surfaces were examined with a systematic rastering technique using sequential fields at relatively low magnification (300-350x), then when particles were seen, higher magnification was used to show morphological characteristics and to do spectral analysis. In this study, images of backscattered or secondary electrons were acquired using 10 kV accelerating voltage, 10 mm working distance, small beam spot, aperture #4, and 60 Pa vacuum (VP-SEM mode). EDS signals were acquired in the spot analysis mode, with dead time <20% and signal counts ~3000-5000 cps. Electron beam penetration depth under the conditions used is estimated to be 2.5 micrometers. Image files were named after the number of EDS site ID, which was consecutive from 1. Spectrum ID was also serial coded consecutively from 1. Once the images or spectra are acquired, the assigned serial ID cannot be changed or replaced.

In studying the blocks of Ms. Converse by SEM/EDS, a total of 4 talc particles were found in a single ~2-micrometer plane of her tissue blocks (see **Table 1** below). All of these were within tissue and were non-fibrous. Two talc particles were found in block 3-4LN (right pelvic lymph node), one in block 2-2C12 (anterior cervix), and one in block 8-3LN (right para-aortic lymph node). The 4 talc particles that were found all had magnesium and silicon in the accepted EDS spectral proportions for talc, i.e. Mg/Si atomic weight % ratios respectively 0.650, 0.639, 0.661, and 0.655 (as shown in **Table 1**) all within ± 5% of the accepted Mg/Si atomic weight % ratio of 0.649 for talc.

In the study of the blocks on this case, a total of 255 particles were analyzed. Tissues may have carbonaceous material detected in backscattered electron imaging mode by their surface irregularity or other characteristics. Also, in many instances iron, sodium, phosphorus, and calcium may be found in tissues, especially in patients with malignancy. These elements are all considered endogenous to the tissues in this type of study. In the tissues studied from Ms. Converse, 95 particles had a calcium composition, either with oxygen alone, or in combination with various endogenous elements. Thirty-five (35) particles had a variety of constituents indicative of exogenous materials including 9 magnesium silicates (sometimes with other cations), and 26 other exogenous particles which included various combinations of metals and/or silicon and/or non-metallic elements. As previously mentioned, the four talc particles (**Table 1** below) that were also found in the tissues all had magnesium and silicon in the accepted EDS spectral proportions for talc.

Table 1: Talc block and spectrum numbers and Mg/Si atomic weight % ratios within ± 5% of 0.649

Block/ spectrum #	Mg/Si ratio
3-4LN 35	0.650
3-4LN 36	0.639
2-2C12 9	0.661
8-3LN 12	0.655

The technique used in the study of Ms. Converse's tissues examines an extremely small volume of tissue. Comparable studies have been done with asbestos fibers in tissue sections (reference 7), and the finding of one fiber in a tissue section comparable to the amount of tissue studied here would indicate at least 100 fibers per gram of tissue, which is indicative of a substantial exposure. If similar approaches were applied to the data from this study, indications are that significant amounts of talc are present: the finding of 4 talc particles spread across 3 out of 7 paraffin

tissue blocks by analytical microscopy, using this approach indicates that a significant amount of talc is present within the patient's tissues. In published studies (references 1, 2, 5, 9), significant numbers of talc particles were detected in pelvic tissues in women with ovarian cancer and a history of perineal talc use.

Figure 4 shows the morphology of representative talc particles detected in this case, and their EDX spectra. The magnesium, silicon, and oxygen peaks are labeled by the software of the instrument, which is periodically checked to assure that known elemental materials are properly identified.

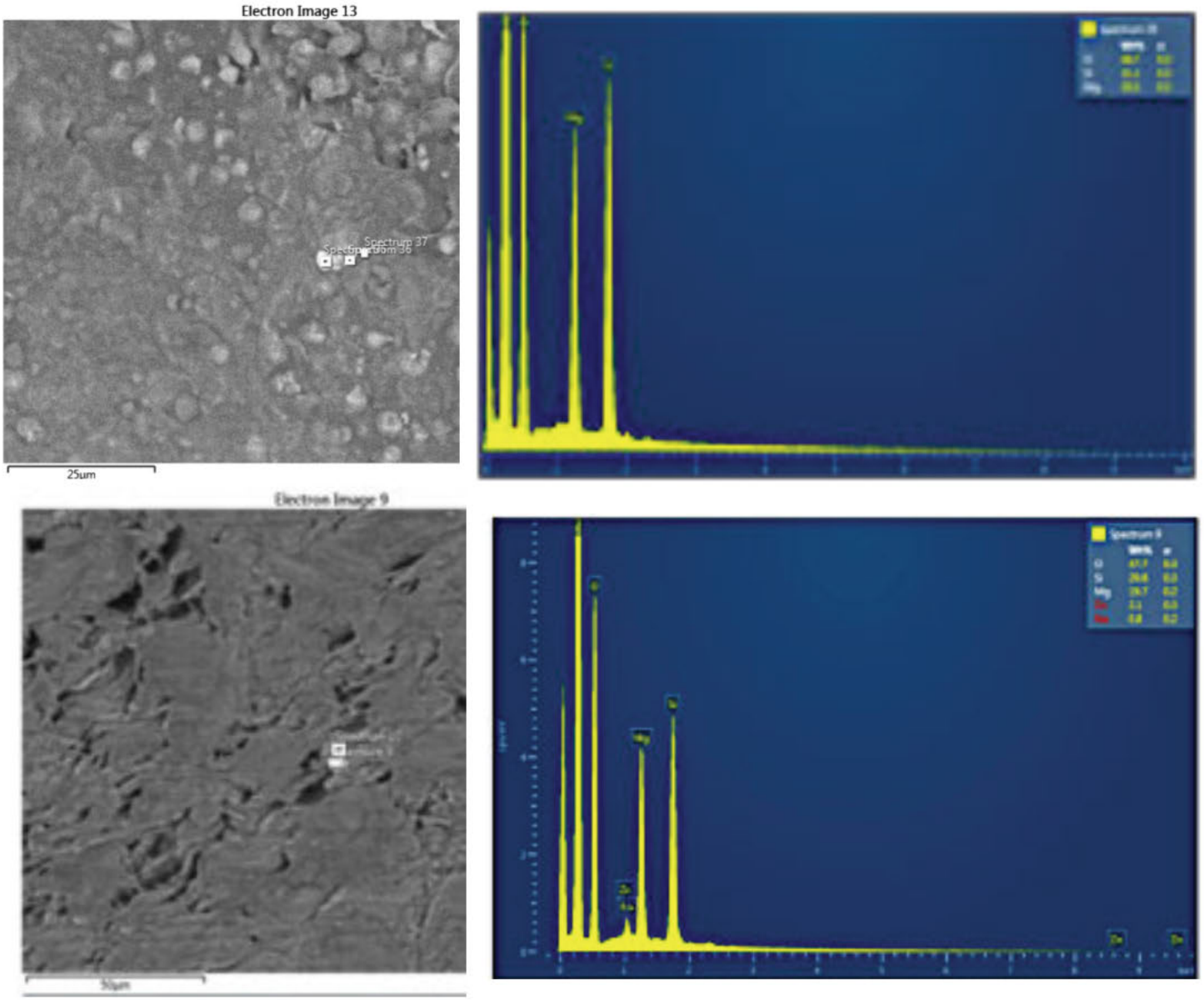

Figure 4. SEM images (left column) and EDS spectra (right column) for the representative talc particles shown here. Respectively, they are: ***Upper*** - block 3-4LN (right pelvic lymph node); and ***Lower*** - block 2-2C12 (anterior cervix). All particles are non-fibrous and in tissue, and are <10 microns in greatest dimension. Their Mg/Si atomic weight % ratios, are 0.650 and 0.661 within ± 5% of the accepted ratio for talc of 0.649, and thus all conforming to the expected spectral proportions for talc. The talc particles in spectra 9 had small components of other cations; this can sometimes be seen in talc particles in tissue with an otherwise unremarkable Mg/Si spectral footprint. The other particles in image 13 (upper) whose spectra are not illustrated included a talc particle spectrum 36 ratio 0.639 and a particle of endogenous composition. and the other particle in electron image 9 (lower) had a magnesium silicate composition (EDS spectra not shown).

Therefore, based on the findings of this case, it can be stated to a reasonable degree of medical certainty, that the talc found in this case is contributory evidence for a causal link between the presence of talc and the development of this patient's ovarian cancer. All opinions expressed in this report are to a reasonable degree of medical and scientific certainty.

Sincerely,

John J. Godleski, MD
Professor Emeritus of Pathology

References:

1. McDonald, SA, Fan Y, Welch, WR, Cramer, DW, Stearns, RC, Sheedy, L, Katler, M, Godleski JJ. Correlative polarizing light and scanning electron microscopy for the assessment of talc in pelvic lymph nodes. Ultrastruct Pathol 43:13-27. 2019. DOI 10.1080/01913123.2019.1593271. PMID: 30898001.

2. McDonald SA, Fan Y, Welch WR, Cramer DW, Godleski JJ. Migration of talc from the perineum to multiple pelvic organ sites: five case studies with correlative light and scanning electron microscopy. Am J Clin Pathol 152: 590-607, 2019. https://doi.org/10.1093/ajcp/aqz080. PMID: 31305893 PMCID: PMC6779257.

3. McDonald SA, Fan Y, Rogers RA, Godleski JJ. Magnesium/silicon atomic weight percent ratio standards for the tissue identification of talc by scanning electron microscopy and energy dispersive X-ray analysis. Ultrastruct Pathol 43: 248-260, 2019. DOI 10.1080/01913123.2019.1692119. PMID: 31736386.

4. Campion A, Smith KJ, Fedulov AV, Gregory DZ, Fan Y, Godleski JJ. Identificatio**n** of Foreign Particles in Human Tissues Using Raman Microscopy Analytical Chemistry 90: (14), 8362-8369, 2018 DOI: 10.1021/acs.analchem.8b00271 PMID:29894163

5. Sato E, McDonald SA, Fan Y, Peterson S, Brain JD, Godleski JJ: Analysis of particles from hamster lungs following pulmonary talc exposures: implications for pathogenicity. Part Fibre Toxicol 2020; 17:20. https://doi.org/10.1186/s12989-020-00356-0. PMID: 32498698 PMCID: PMC7271432.

6. Johnson KE, Popratiloff A, Fan Y, McDonald S, Godleski JJ. Analytic comparison of talc in commercially available baby powder and in pelvic tissues resected from ovarian carcinoma patients. Gynecol Oncol 2020; 159: 527-533. PMID: 32977988.

7. Abraham JL, Thakral C. Automated scanning electron microscopy and X-ray microanalysis for in situ quantification of gadolinium deposits in skin. Microscopy 2007; 56: 181-187. PMID: 17951398.

8. Roggli VL, Pratt PC. Numbers of asbestos bodies on iron-stained tissue sections in relation to asbestos body counts in lung tissue digests. Hum Pathol 1983; 14: 355-361. PMID: 6299925.

9. Cramer DW, Welch WR, Berkowitz RS, Godleski JJ. Presence of talc in pelvic lymph nodes of a woman with ovarian cancer and long-term genital exposure to cosmetic talc. Obstet Gynecol 2007; 110: 498-501. PMID: